Eur. Radiol. (2001) 11: 1374–1388
DOI 10.1007/s003300100845

Carlo Bartolozzi
Dania Cioni
Francescamaria Donati
Riccardo Lencioni

Focal liver lesions: MR imaging–pathologic correlation

Received: 27 December 2000
Accepted: 15 January 2001
Published online: 20 March 2001

C. Bartolozzi (✉) · D. Cioni · F. Donati · R. Lencioni
Division of Diagnostic and Interventional Radiology, Department of Oncology, Transplants, and Advanced Technologies in Medicine, University of Pisa, Via Roma 67, 56100 Pisa, Italy
E-mail: Bartolozzi@do.med.unipi.it
Phone: +39-050-992509
Fax: +39-050-551461

Abstract Magnetic resonance signal intensity of focal liver lesions is affected by numerous pathologic factors. Lesion histologic features, such as cellularity, vascularity, stromal component, and intratumoral necrosis or hemorrhage, strongly affect T1 and T2 relaxation times. Additionally, intracellular content of certain substances, such as glycogen, fat, melanin, iron, and copper, may also have a substantial role in determining MR signal behavior. In this review we discuss the correlations between MR imaging features and pathologic findings in benign and malignant focal liver lesions. Knowledge of imaging–pathology correlations greatly assist in characterizing focal lesions. Moreover, in certain tumor histotypes, such as hepatocellular carcinoma, careful analysis of lesion signal intensity may help predict the degree of tumor differentiation.

Keywords Liver · Liver neoplasms · MR imaging Diagnosis

Introduction

Magnetic resonance signal intensity of focal liver lesions depends on both histologic and cytologic features [1, 2, 3]. Among histologic characteristics, hypercellularity and hypervascular supply are usually associated with low signal intensity on T1-weighted images and high signal intensity on T2-weighted images. The stromal (fibrous) component, in contrast, reduces signal intensity on T2-weighted images. Necrotic areas may exhibit different features, depending on the type of the necrosis itself: Whereas liquefactive necrosis is highly hypointense on T1-weighted images and highly hyperintense on T2-weighted images by virtue of the increased water content, coagulative (dehydrated) necrosis shows the opposite behavior, being characterized by low signal intensity on T2-weighted images. Hemorrhagic areas may show different patterns, depending on the timing of the bleeding: The most common appearance is that of hyperintensity on T1-weighted images, caused by extracellular metahemoglobine (Fig. 1).

Intracytoplasmatic accumulation of glycogen or fat may shorten T1 relaxation time of lesions increasing signal intensity on T1-weighted images (Fig. 2) [4]. Melanin also has paramagnetic properties which increase the signal intensity on T1-weighted images. While intratumoral content of copper usually has limited influence on MR signal intensity of liver lesions, iron deposits may greatly reduce signal intensity, especially on T2-weighted images (Fig. 3) [5]. In hepatocellular lesions, the presence of Kupffer's cells and the degree of hepatocyte-like function influence MR signal intensity in images obtained after administration of tissue-specific MR contrast agents, such as reticuloendothelial-system-targeted agents and hepatobiliary agents [6, 7].

The signal intensity of a focal lesion on MR images is the outcome of its different histologic and cytologic features. Careful analysis of lesion signal intensity on MR images, therefore, is crucial for proper characterization of focal lesions [1, 2, 3]. In this article we review the MR imaging features of the most common benign and malignant liver lesions, highlighting imaging–pathology correlations.

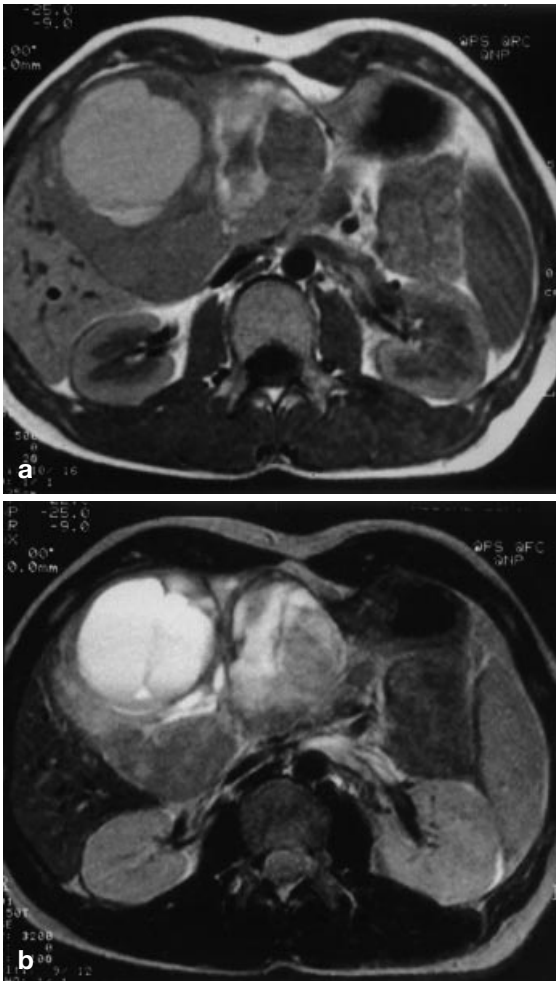

Fig. 1 Subacute intratumoral bleeding, associated with extracellular metahemoglobine, gives a markedly high signal intensity both on **a** T1- and **b** T2-weighted MR images

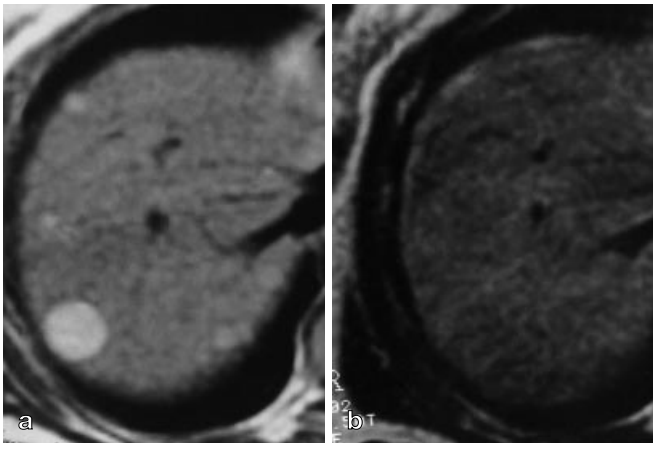

Fig. 2 **a** Glycogen accumulation within macroregenerative nodules in cirrhosis give a markedly high signal intensity on T1-weighted MR images. **b** The lesions are isointense to liver on T2-weighted image

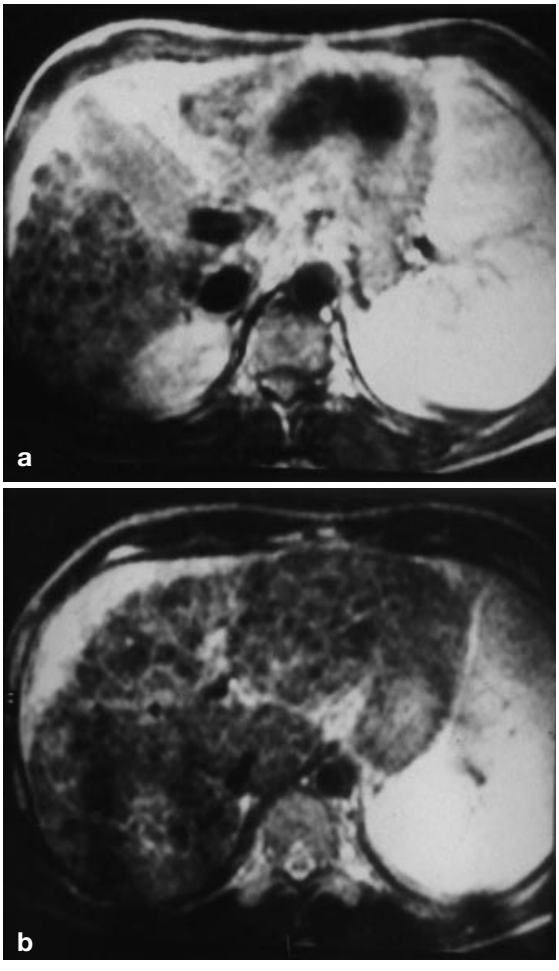

Fig. 3 a, b Iron deposits within macroregenerative nodules involving the whole liver parenchyma give a markedly low signal intensity on T2-weighted MR images

Benign liver lesions

Hemangioma

Hemangioma is the most common benign liver tumor, with a prevalence of up to 7–20 % in autopsy series. It is usually asymptomatic and incidentally detected. Hemangiomas are well-circumscribed, blood-filled masses of variable size. On cut sections, areas of fibrosis, hemorrhage, or thrombosis may be seen, especially in large hemangiomas. The blood-filled spaces or vascular channels that comprise hemangiomas are lined by a single layer of endothelial cells. The channels themselves are separated by thin, fibrous septa, which may form finger-like projections into the channels.

Owing to the high blood (water) content, hemangiomas appear as hypointense lesions on T1-weighted images and as markedly hyperintense lesions on T2-

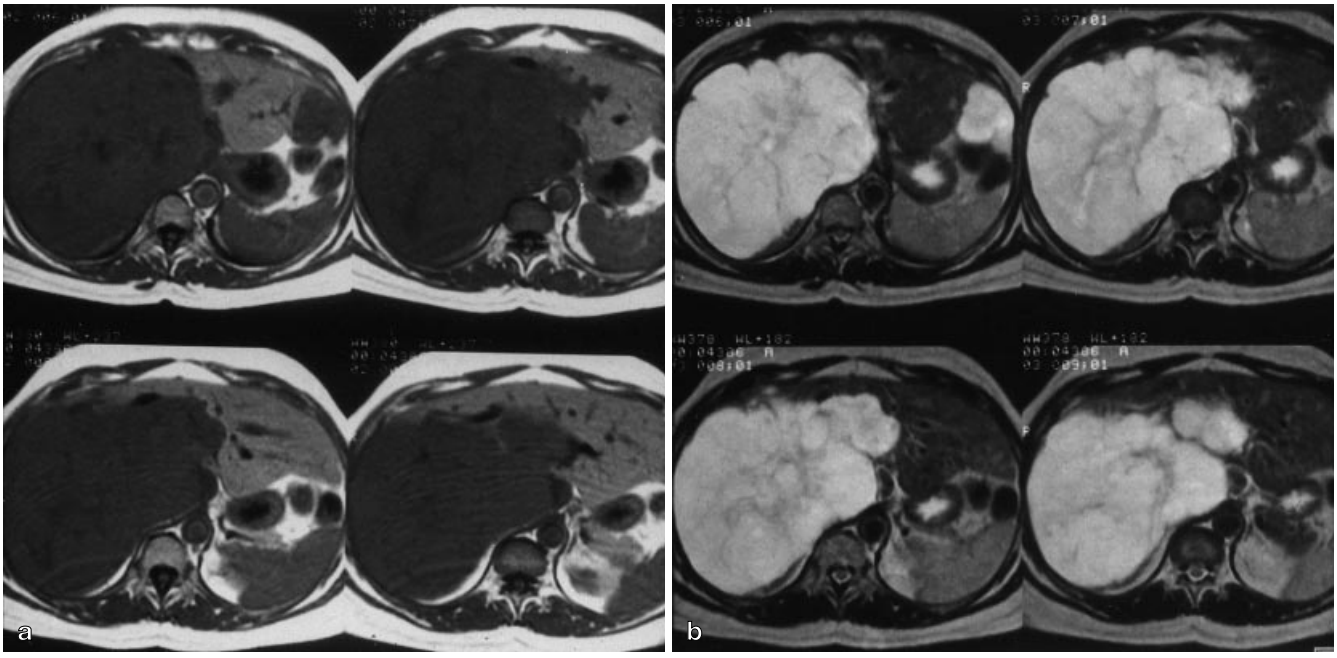

Fig. 4 a, b Giant hemangioma. **a** On T1-weighted images the lesions appear definitely hypointense, whereas it is markedly bright on **b** T2-weighted images. Internal areas of fibrosis are detected as low-intensity bands both on T1- and T2-weighted images

weighted images. Imaging with heavily T2-weighted sequences, in fact, enhances the ability to differentiate hemangiomas from malignant tumors [8]. Low-intensity areas on T2-weighted images may sometimes be seen in the central portion of large hemangiomas, being usually associated with fibrosis (Fig. 4).

Dynamic MRI with extracellular contrast agent administration may display the slow perfusion pattern of hemangioma, showing peripheral nodular enhancement in the early phase, progressing centripetally to uniform (or almost uniform) enhancement in the delayed phase. Persistent hypointensity, in fact, is frequently seen in the central portion of large hemangiomas owing to fibrotic or thrombotic phenomena. Small (< 1.5-cm) hemangiomas, however, may show uniform enhancement in the arterial phase, which tend to persist in the delayed phase (Fig. 5) [9, 10, 11]. Hemangiomas may show increased signal intensity on T1-weighted images even after administration of superparamagnetic contrast agents, due to the T1 effect of the agent trapped within the vascular lacunae of the lesion [12].

Focal nodular hyperplasia

Focal nodular hyperplasia (FNH) accounts for approximately 8 % of all primary hepatic tumors and represents the second most common benign liver tumor after hemangioma. Most FNHs are seen in women in the third to fifth decades of life. Focal nodular hyperplasia arises as a localized hepatocyte hyperplastic response to an underlying congenital vascular malformation. Focal nodular hyperplasia may be associated with hemangiomas. The use of oral contraceptives is associated with FNH; however, it only promotes the growth of the lesion and does not induce its formation.

Focal nodular hyperplasia is a well-circumscribed mass, lacking a true capsule, and is characterized by a central scar of vascular connective tissue with prominent arterial vessels that extend outward, through fibrous septa, to the periphery of the tumor. These septa circumscribe nodules of hepatocytes and small bile ducts. Kupffer's cells are also present. The lesion does not show internal hemorrhage or necrosis: The growth of FNH, in fact, remains proportional to its blood supply. Of interest, FNH has an exclusive arterial blood supply, with no portal vein branches [13, 14].

Focal nodular hyperplasia is essentially a hyperplastic process, in which all the components of normal liver are present although abnormally organized. These pathologic features explain the typical MR appearance of this lesion. Focal nodular hyperplasia, in fact, is usually isointense or nearly isointense with respect to normal liver parenchyma both on T1- and T2-weighted images. The central scar, made by water-rich vascular connective tissue, appears hypointense on T1-weighted images and hyperintense on T2-weighted images [10, 15, 16, 17, 18].

After administration of an extracellular contrast agent, FNH demonstrates a peculiar behavior: In the

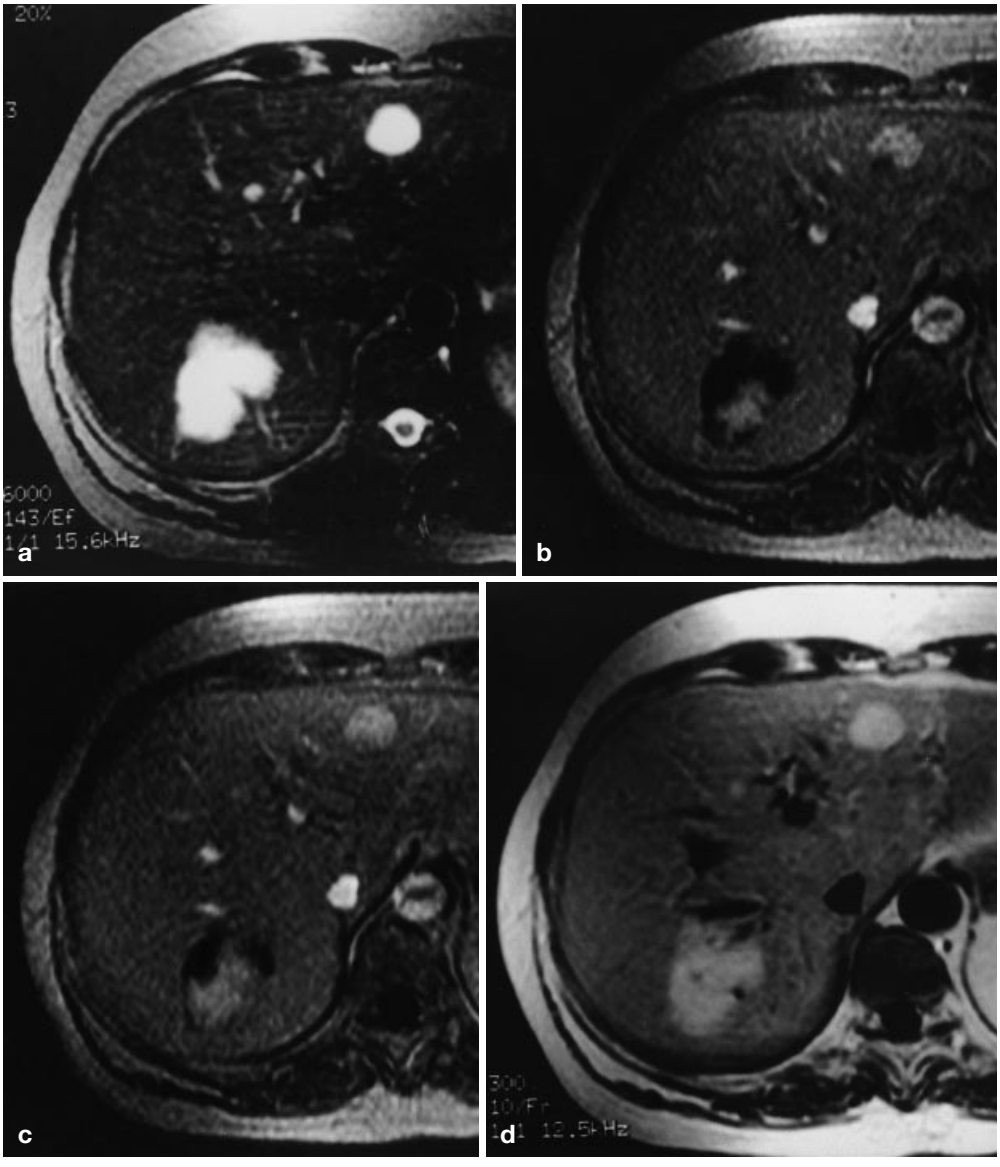

Fig. 5 a–d Hepatic hemangiomas. **a** On the T2-weighted image, two hemangiomas are detected as markedly hyperintense lesions. During the dynamic, gadolinium-enhanced study (**b** arterial phase; **c** portal venous phase; **d** delayed phase), the largest lesion shows peripheral nodular enhancement in the early phase progressing centripetally to uniform enhancement in the delayed phase. The smaller lesion, in contrast, demonstrates uniform enhancement in the arterial phase, which persists in the portal and the delayed phases

arterial phase, the lesion shows clear-cut enhancement, with the central scar being unenhanced (Fig. 6). In the portal phase, the lesion undergoes rapid washout of contrast, becoming isointense to liver. The central scar may show delayed enhancement, particularly in medium-to-large-sized lesions [10, 19, 20].

After administration of reticuloendothelial-system-targeted agents, FNH, owing to the presence of Kupffer cells, shows signal intensity loss on T2-weighted images, similar to that of normal hepatic parenchyma, sparing the central scar [12]. Contrast uptake is also seen after injection of hepatobiliary agents, with variable signal intensity increase on T1-weighted images [6, 21, 22].

Hepatocellular adenoma

Hepatocellular adenoma (HCA) is an uncommon primary benign tumor. The incidence of HCA increased following the introduction of oral contraceptives, and oral contraceptives and androgen steroids therapy have been identified as definitive causative agents. Hepatocellular adenoma can also occur spontaneously or be associated with underlying metabolic disease. The diagnosis of this entity is clinically important because it can bleed, causing life-threatening hemorrhage, and because it has a potential, although very rare, for malignant transformation.

Hepatocellular adenoma presents as a solitary lesion in most cases and is typically a well-circumscribed tu-

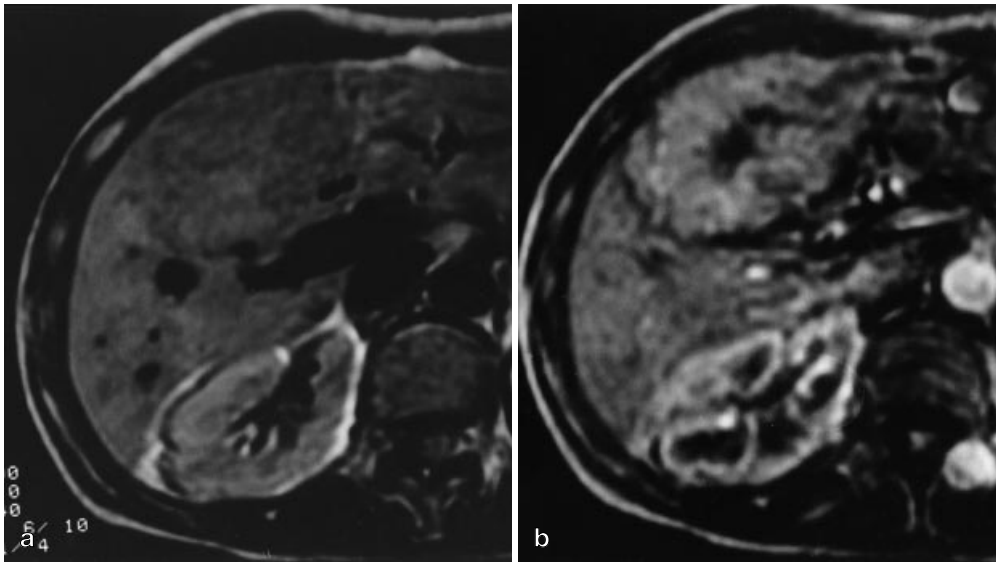

Fig. 6 a, b Focal nodular hyperplasia. **a** The lesion is nearly isointense to liver in the proton density-weighted MR image, with inhomogenously hyperintense central scar. **b** On the contrast-enhanced T1-weighted image acquired in the arterial phase, the lesion demonstrates clear-cut enhancement, sparing the central scar

mor. The presence of large subcapsular arterial vessels accounts for its typical hypervascular nature. Hepatocellular adenoma has a propensity to outgrow its vascular supply, resulting in hemorrhage and occasionally rupture. Histologically, HCA is composed of cords of hepatocytes. Although the hepatocytes can produce bile, there are no bile ducts present to enable biliary excretion. The hepatocytes contain increased amounts of glycogen and sometimes fat [14].

The rich intracellular content of glycogen is the main element responsible for the increased signal intensity of HCA on T1-weighted images with respect to surrounding liver parenchyma. Areas of internal hemorrhage are typically depicted as markedly hyperintense areas on T1-weighted images, owing to the presence of extracellular metahemoglobine.

In dynamic contrast-enhanced MR studies, HCA shows early enhancement during the arterial phase, reflecting its hypervascularity, with rapid washout [23, 24]. Hepatocellular adenoma may also take up hepatobiliary agents and appear hyperintense with respect to the liver parenchyma on T1-weighted images [6, 21, 22].

Angiomyolipoma

Angiomyolipomas are rarely encountered in the liver, and can occur as solitary mass or as multiple lesions in association with tuberous sclerosis. They are composed of variable amounts of fat, smooth muscle cells, and vessels [25, 26]. The fatty nature of the tumor results in an hyperintense appearance on T1-weighted images [27]. The use of fat-suppressed or out-of-phase MR images can help in characterizing angiomyolipomas, showing signal intensity loss (Fig. 7) [28].

Macroregenerative and dysplastic nodules

Macroregenerative and dysplastic nodules typically arise in livers with chronic disease. They consist of hyperplastic or dysplastic hepatocytes, and may have malignant potential [29, 30, 31, 32, 33, 34]. They appear as small (< 2 cm) nodular lesions that are hyperintense or isointense on T1-weighted images and hypointense or isointense on T2-weighted images relative to the surrounding liver (Fig. 8). The increased signal intensity on T1-weighted images may be due to the increased intracellular content of glycogen, and resembles the appearance of well-differentiated hepatocellular tumors [9, 35]. Nodules with a malignant focus may show a nodule-within-a-nodule appearance.

Malignant liver lesions

Hepatocellular carcinoma

Hepatocellular carcinoma (HCC) is a common malignancy throughout the world, with an estimated incidence of up to 1,000,000 new cases per year. The highest incidence rates are found in sub-Saharan Africa and the Far East. Areas of low incidence include North America and Northern Europe, whereas Mediterranean countries have an intermediate-to-high incidence. The geographic distribution of HCC is related to the etiology of the disease: In Western countries and in the Far East, most cases occur in patients with liver cirrhosis, following hepatitis B or C infection [1].

On gross pathology, most HCCs fall into one of two categories. The nodular form, which is characterized by the presence of one or more encapsulated or non-en-

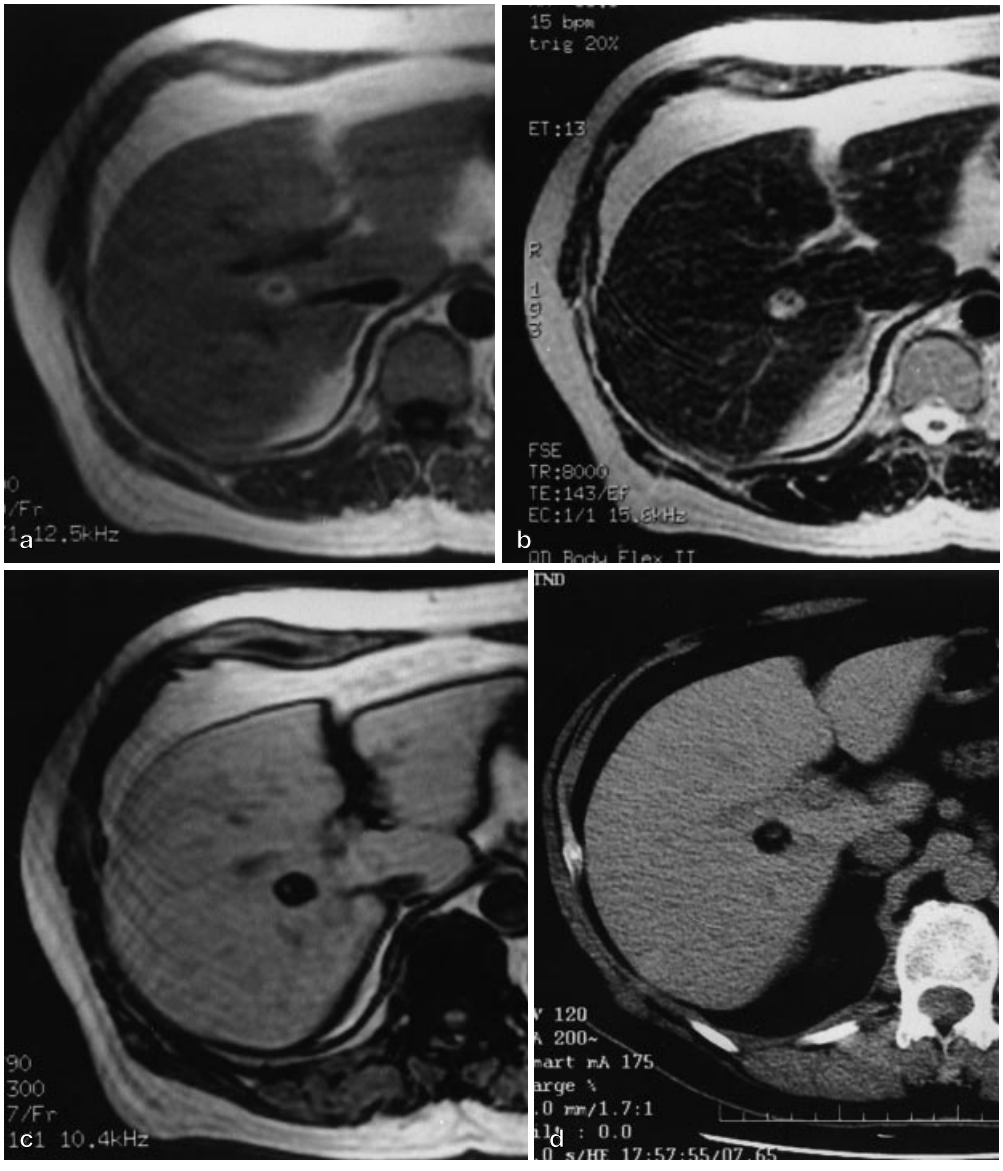

Fig. 7a–d Angiomyolipoma. The lesion appears as a hyperintense nodule both on **a** T1- and **b** T2-weighted MR images, with a small central hypointense area. **c** Out-of-phase gradient-echo MR image shows definite signal intensity loss. **d** The fatty nature of the lesion is confirmed by its hypodensity, with negative attenuation values, on unenhanced CT

capsulated nodules, is seen predominantly in cirrhotic livers. The massive form, which consists in a large solitary and infiltrating tumor, is more frequent in developing countries, and, in most cases, there is no underlying cirrhosis. There is also a third so-called diffuse form, which is much less common than either of the former forms and is characterized by miliary infiltration of liver parenchyma. Four histologic patterns are distinguished: trabecular; pseudo-glandular; solid; and scirrhous (or sclerosing). Depending on the cellular characteristics, these tumors are also described as well-differentiated, moderately differentiated, poorly differentiated, or undifferentiated (anaplastic) [36].

The histologic pattern, the degree of tumor differentiation, the amount of fibrosis, the presence of internal necrosis or hemorrhage, as well as the intracellular content of glycogen, fat, or metal ions greatly affect the MR appearance of the lesion [5, 37, 38, 39]. Nodular-type HCC is often well defined, possibly encapsulated. In contrast, the diffuse form of HCC is poorly marginated and shows an infiltrative pattern, with a high tendency to invade the portal vein branches. The signal intensity of HCC may be inhomogeneous and vary greatly, especially in the nodular form. The appearance may range from hypointense to iso- or hyperintense on T1-weighted images and from isointense to hyperintense on T2-weighted images. Usually, hyperintensity on T1-weighted images and isointensity on T2-weighted images are associated with well-differentiated tumors (Fig. 9) [40, 41, 42, 32]. High signal intensity on T1 may

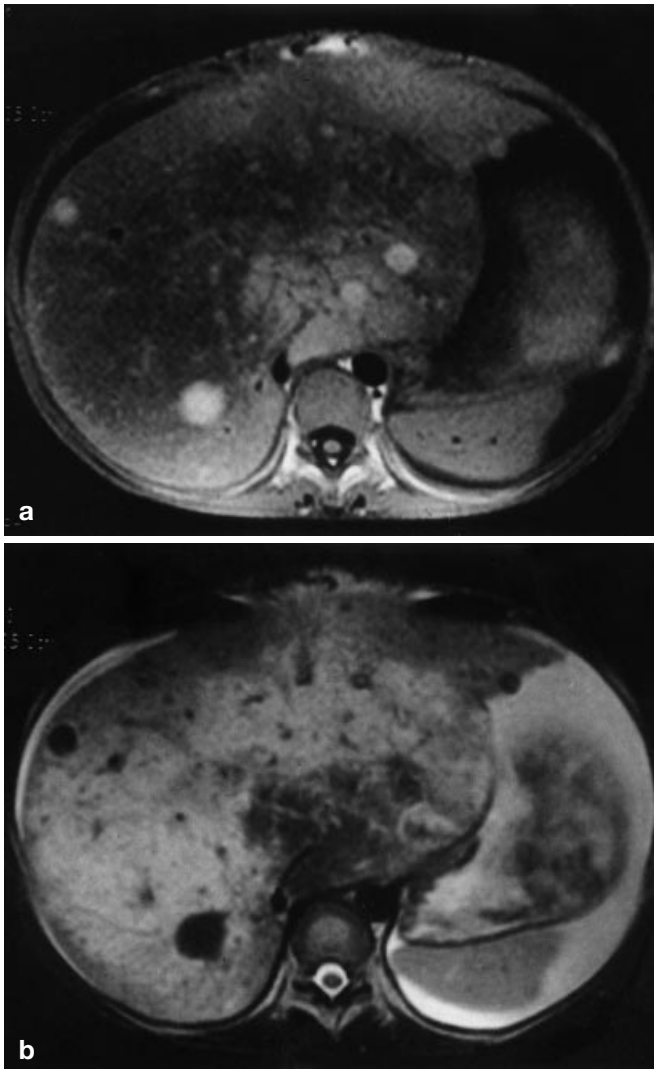

Fig. 8 a, b Macroregenerative nodules in Budd-Chiari syndrome. **a** T1-weighted image shows multiple, small, hyperintense nodular lesions within the diseased liver. **b** On the T2-weighted image, the lesions appear markedly hypointense

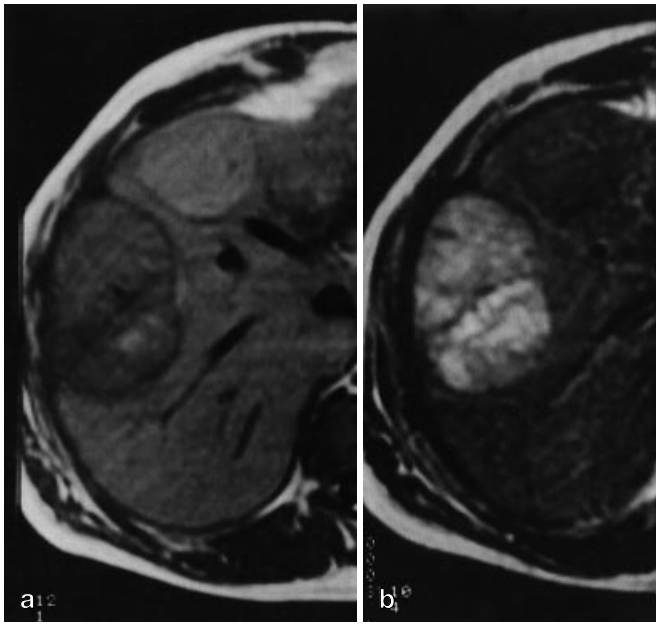

Fig. 9 a, b Multinodular hepatocellular carcinoma. **a** The T1-weighted MR image shows two lesions with different signal intensity: The larger tumor is hypointense to liver, whereas the smaller one is hyperintense. **b** On the T2-weighted image, the larger nodule is hyperintense, whereas the smaller one is isointense compared with surrounding liver parenchyma. Histology showed moderately differentiated hepatocellular carcinoma in the larger lesion and well-differentiated hepatocellular carcinoma in the smaller lesion

be due to the rich intracellular content of glycogen or fat, probably reflecting a defective release of these components by partially functioning hepatocytes [4, 43, 44].

Numerous additional findings may be visualized with MRI [42]. Tumor capsule is depicted as a thin rim with hypointense signal intensity on T1-weighted images due to its fibrotic composition. T2-weighted images delineate a single ring with hypointense signal intensity or a double ring with inner hypointensity and outer hyperintensity. Histopathology reveals two-layered capsules with a thin fibrous inner zone and an outer zone that consists of compressed small vessels and bile ducts. A mosaic pattern is a common MRI finding in HCC [45]. Intratumoral, linear-like hypointense areas are detected on T1-weighted images and a nonuniform signal on T2-weighted images. Histopathologic correlation reveals intratumoral septa and a variety of histopathologic findings within the tumorous tissue. Central necrosis presents usually with hypointensity on T1-weighted images, with marked hyperintensity on T2-weighted images in the case of liquification. Hyperintense foci inside the nodules on T2-weighed images are likely to represent intratumoral sinusoidal dilation due to peliotic change.

Hepatocellular carcinoma is typically nourished by the hepatic artery and this elective vascularization can be demonstrated by dynamic contrast-enhanced MRI [46, 47, 48, 49]. Hepatocellular carcinoma typically shows peak of contrast uptake in the arterial phase of the dynamic MR study, corresponding to the arteriographic finding of neovascularity or staining (Fig. 10) [50, 51, 52, 53, 54, 55, 56]. Well-differentiated tumors, however, may not exhibit the typical hypervascularity of overt HCC and show slight progressive enhancement with no peak in the arterial phase [36, 37, 57]. Sclerosing HCC can show some delayed enhancement due to the abundant fibrous component [49, 58].

The contrast behavior of HCC after administration of hepatobiliary agents is dependent on the degree of

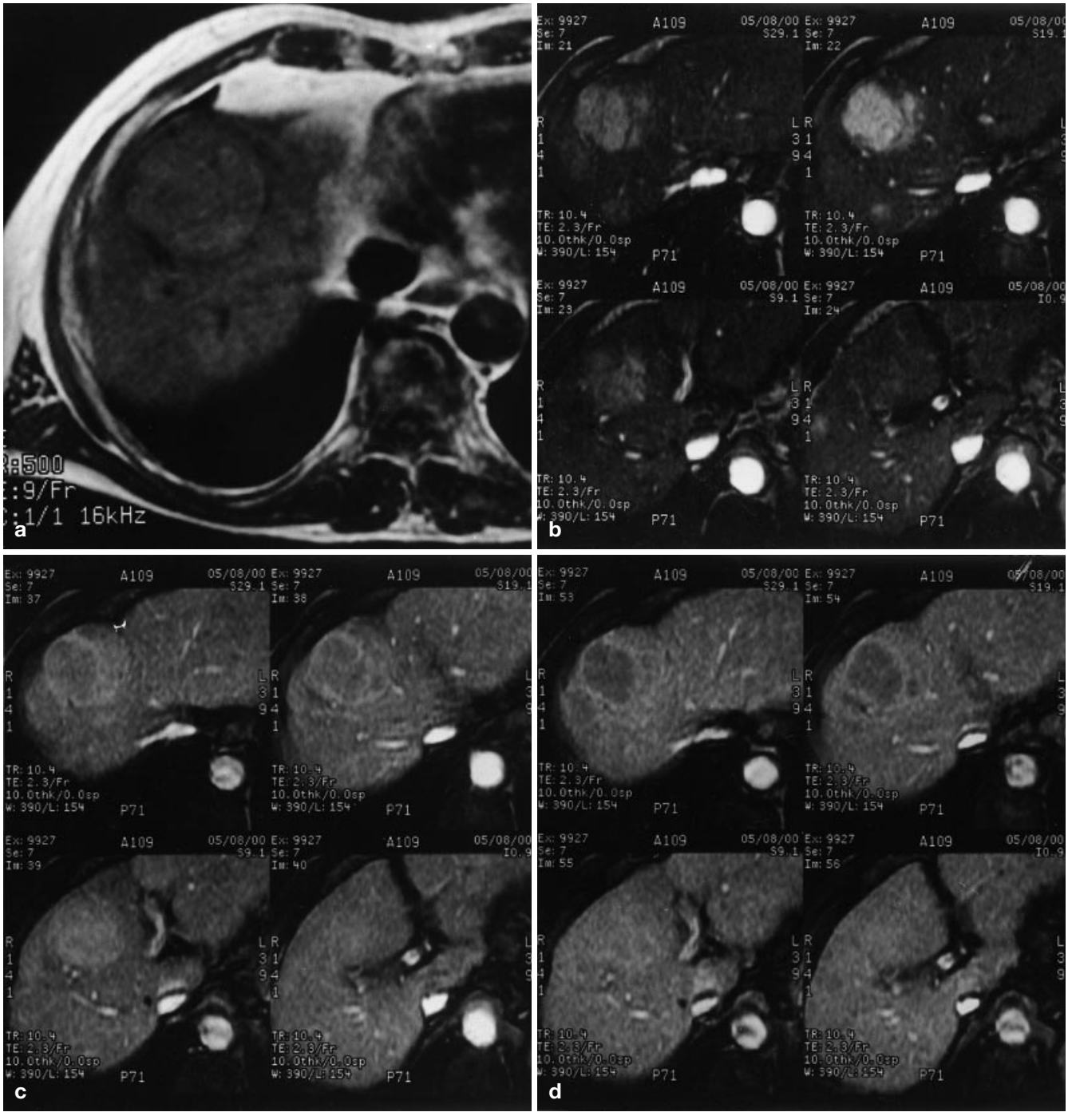

Fig. 10 a–d Hepatocellular carcinoma with satellite lesions. **a** The T1-weighted MR image shows a nodular lesion which is slightly hyperintense with a hypointense peripheral rim. During the dynamic, gadolinium-enhanced study (**b** arterial phase; **c** portal venous phase; **d** delayed phase), the tumor shows clear-cut enhancement in the early phase with rapid washout. Small satellite nodules become visible around the tumor, and show the same enhancement pattern as the main lesion

differentiation of tumor cells: Whereas moderately or poorly differentiated lesions fail to take up hepatobiliary agents and appear hypointense to liver on enhanced images, well-differentiated tumor may show the opposite behavior, appearing hyperintense with respect to liver parenchyma as a result of the uptake and trapping of the agent within the tumor [6, 7, 59, 60].

Cholangiocellular carcinoma

Cholangiocellular carcinoma is a primary malignancy arising from the bile duct epithelium. The incidence of cholangiocellular carcinoma among primary liver cancer usually does not exceed 10 % of cases. It is a disease of older individuals and occurs slightly more frequently in males than females. According to the site of origin, cholangiocellular carcinoma is classified into two types: intrahepatic and extrahepatic. The term cholangiocarcinoma should be used for intrahepatic lesions, whereas bile duct carcinoma should be preferred for extrahepatic neoplasms [61].

The intrahepatic or peripheral cholangiocarcinoma represents 10 % of all cholangiocarcinomas. It arises from the internal wall of the small bile ducts, peripheral to the right or left hepatic ducts, and grows into the liver as a focal mass. The gross appearance of cholangiocarcinoma is that of grayish white, firm, solid, and fibrous mass. Characteristically, this malignancy has a large central core of fibrotic tissue, due to the desmoplastic reaction provoked by the neoplastic cells. Microscopically, cholangiocarcinoma represent an adenocarcinoma with glandular appearance. Mucus secretion and calcification are sometimes found, but there is no bile production [61].

The MR appearance of cholangiocarcinoma is that of a non-capsulated tumor, hypointense on T1-weighted images and hyperintense on T2-weighted images. Dilatation of the peripheral portion of the intrahepatic biliary ducts may be seen. The signal intensity of the tumor is variable according to the amount of fibrosis, necrosis, and mucinous material within the tumor. Central hypointensity may be seen on T2-weighted images, corresponding to central areas of fibrosis [62, 63, 64]. On dynamic contrast-enhanced MR studies, minimal to moderate peripheral enhancement is evident followed by progressive filling. Pooling of contrast within the tumor, reflecting the large amount of fibrous tissue, is typically seen on delayed MR images (Fig. 11) [65, 66, 67].

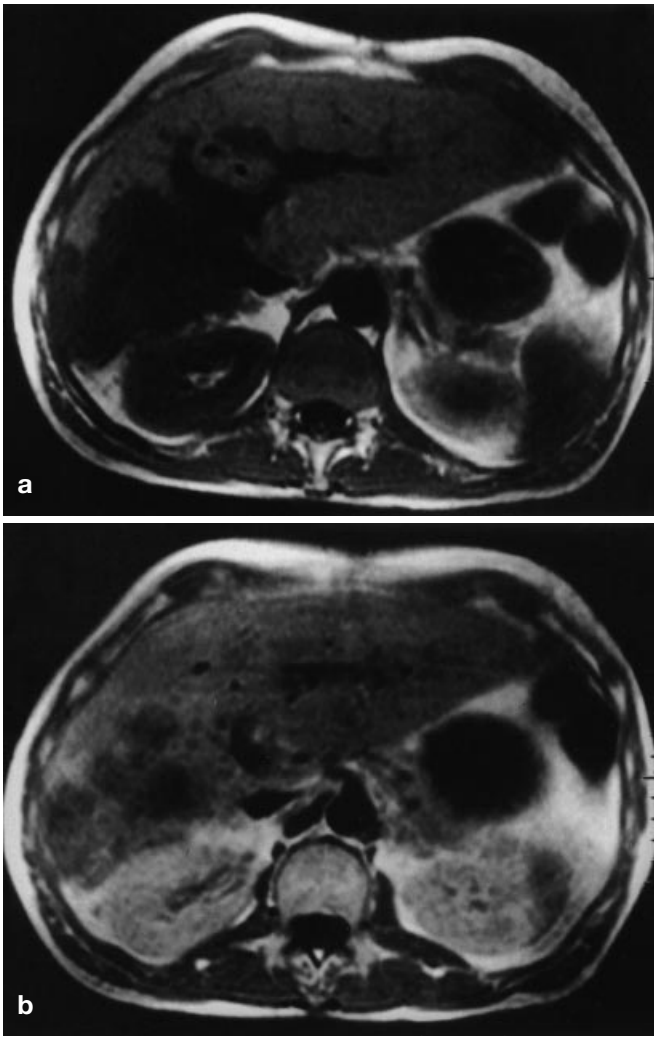

Fig. 11 a, b Intrahepatic cholangiocellular carcinoma. **a** The tumor is hypointense to liver on the T1-weighted image. **b** Pooling of contrast within the tumor, reflecting the large amount of fibrous tissue, is seen on the delayed, gadolinium-enhanced image

Fibrolamellar carcinoma

Fibrolamellar carcinoma is a rare neoplasm of hepatocellular origin that was considered in the past a variant of HCC, whereas it is now seen as an independent entity. In contrast to HCC, fibrolamellar carcinoma is seen in young patients without cirrhosis. Pathologically, this tumor usually presents as a large solitary mass with a lobulated contour and a central fibrous scar that may be calcified. Calcification is central, stellate, or nodular, and the amount of calcification is usually small relative to the large size. Satellite nodules may also be present. Abundance of fibrosis distributed in bands or laminae (hence fibrolamellar) is a hallmark of this neoplasm [68, 69, 70, 71, 72].

Magnetic resonance imaging reveals the tumor with a partial or complete capsule. In general, tumors are iso- or hypointense to the liver on T1-weighted images and iso- to hyperintense on T2-weighted images. The scar may have low signal intensity on both T1- and T2-weighted images, although cases of hyperintense scars on T2-weighted images have been reported [73, 74]. The tumor is not as vascularized as HCC.

Epithelioid hemangioendothelioma

Epithelioid hemangioendothelioma (EHE) is a rare malignant hepatic neoplasm of vascular origin that develops in adults. It should not be confused with infantile

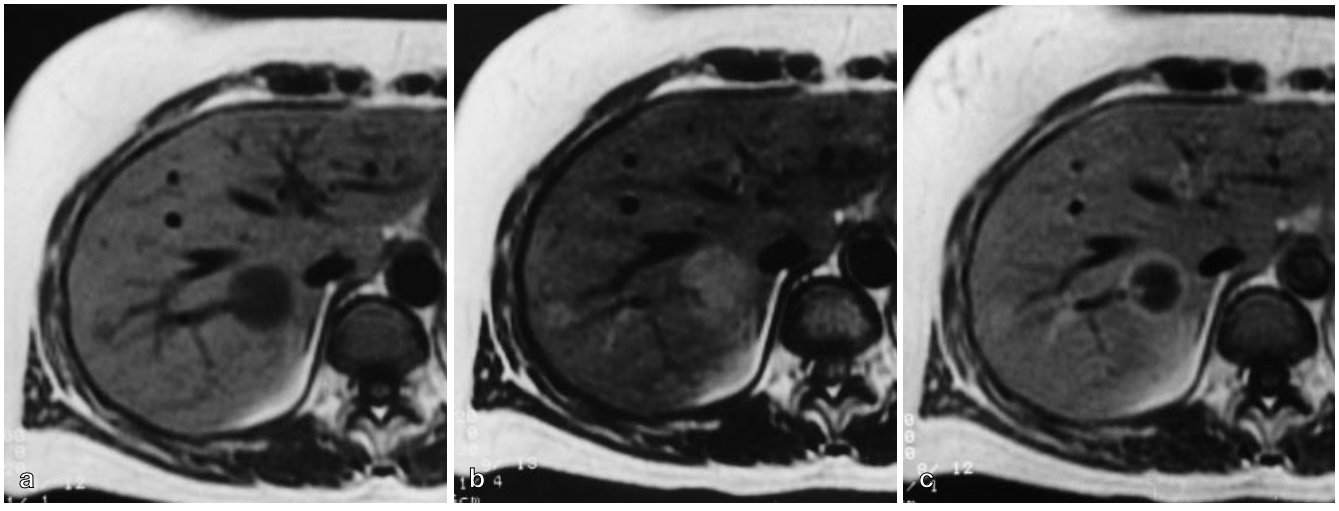

Fig. 12 a–c Epithelioid hemangioendothelioma. **a** On the T1-weighted image, two hypointense nodules are detected. **b** The lesions appear hyperintense on the T2-weigted image. **c** Delayed contrast-enhanced T1-weighted image shows peripheral, rim-like enhancement in the larger lesion, and homogeneous enhancement in the smaller lesion

hemangioendothelioma. Only recently has EHE been recognized as a distinct entity. It is a solid tumor composed primarily of epithelioid-appearing endothelial cells. The tumor has a variable clinical course between that of benign endothelial tumors (hemangiomas) and malignant angiosarcomas. Unlike most primary malignant hepatic tumors, two-thirds of patients affected are women, in the third of fourth decades of life. No risk factors of specific causes of hepatic EHE are known [75, 76].

Macroscopically, multifocal nodules varying in size from a few millimeters to several centimeters are seen. These nodules tend to coalesce, as they grow, to form large confluent masses, usually in the periphery of the liver, owing to the extension of the tumor through the tributaries of the portal and hepatic veins. These solid tumors characteristically have a dense fibrotic hypovascular central core and a peripheral hyperemic rim. The hepatic capsule overlying an EHE is frequently retracted inward, which is thought to be due to fibrosis induced by the tumor. This capsular retraction is an unusual feature in malignant lesions of the liver, and is suggestive of EHE [77].

Microscopically, the tumors are composed of dendritic spindle cells and epithelioid round cells within abundant matrix of myxoid and fibrous stroma. Neoplastic cells invade and eventually obliterate sinusoids, terminal hepatic veins, and portal veins. Approximately 30% of patients may demonstrate progressive sclerosis and eventual calcification [76, 77].

Concentric alteration in signal intensity, corresponding to the regions of different histology, are seen both on T1- and T2-weighted images. The MR images demonstrate subcapsular nodules of increased signal intensity on T2-weighted images similar to that of most malignancies, but not as intense as the characterizing high signal intensity of hepatic hemangiomas. Peripheral, rim-like enhancement is seen after administration of extracellular contrast agents (Fig. 12) [76, 78].

Angiosarcoma

Angiosarcomas are malignant neoplasms derived from endothelial cells that occurs primarily in adults with exposure to a variety of chemical agents and radiation. Although primary angiosarcoma accounts for less than 2% of all primary liver neoplasms, it is the most common sarcoma of the liver.

Primary hepatic angiosarcomas are highly aggressive and have an extremely poor prognosis. It occurs four times more frequently in males [79]. Macroscopically, there are two patterns of growth: multifocal nodules and large solitary mass. The tumor nodules varies in size from pinpoint foci to large nodules measuring several centimeters in diameter. The nodules may have a dark, red-brown appearance due to the presence of areas of internal hemorrhage. When angiosarcoma appears as a solitary, large mass, it does not have a capsule and frequently contains large cystic areas filled with blood debris.

Microscopically, hepatic angiosarcomas are composed of malignant vascular cells that may form poorly organized vessels, variable in size from cavernous to capillary, trying to form sinusoids. These vessels are lined with malignant endothelial cells. Tumor cells tend to grow along preformed vascular channels, particularly the sinusoid, and may form solid nodules or cavitary spaces [79].

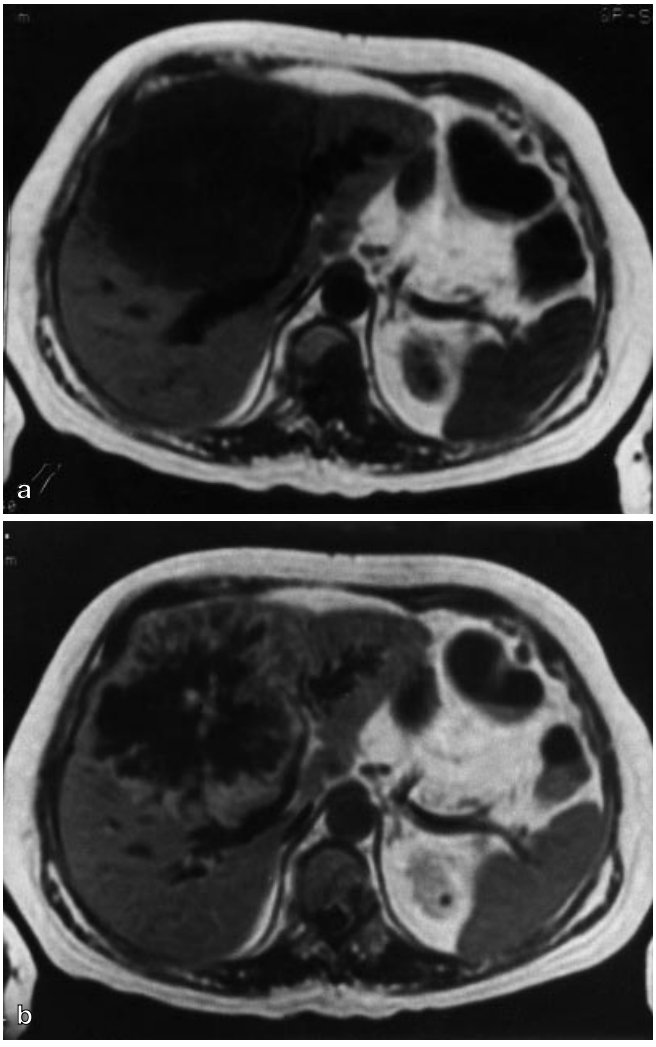

Fig. 13a, b Angiosarcoma. **a** The tumor is hypointense to liver on the T1-weighted image. **b** Inhomogeneous peripheral enhancement, without nodular pattern, is seen on the gadolinium-enhanced image

With MR imaging, the signal intensity features of angiosarcoma are similar to those sometimes seen in hemangioma. Both tumors contain abundant blood-filled vascular spaces, which may exhibit high signal intensity on T2-weighted MR images. Peripheral enhancement after extracellular contrast agent administration may be seen, but it is not of the dense, discontinuous, and globular pattern that is typically seen in cases of hemangioma (Fig. 13) [80].

Lymphoma

Primary hepatic lymphoma is a rare disease. Lymphoma is considered to be a primary neoplasm of the liver when the tumor is limited to hepatic parenchyma. Grossly, nodular and diffuse forms of hepatic lymphoma are seen. Hodgkin's disease occurs more often as miliary lesions than masses: Early in the disease liver parenchyma involvement is microscopic, but with time, small nodules from a few millimeters to several centimeters in size develop. In non-Hodgkin's lymphoma, the lymphocytic form tends to be miliary, whereas the large cells or histiocytic varieties are nodular masses [81, 82].

On MR images these tumors are hypointense on T1-weighted images and hyperintense on T2-weighted images due to the rich cellularity [16, 83, 84]. After administration of extracellular contrast agents, these tumors remain hypointense during all the dynamic study, due to their poor vascularity (Fig. 14) [1].

Liver metastases

Metastatic disease involving the liver represents one of the most common problems in oncology. The liver provides a fertile soil for metastases, not only due to its dual blood supply from both systemic and splanchnic system, but also because of the presence of humoral factors promoting cell growth and the discontinuous nature of endothelial lining of the hepatic sinusoid allowing open communication with the extracellular space of Disse. The liver is second only to regional lymph nodes as a site of metastatic disease. The true prevalence of metastatic disease is unknown, because most figures are based on autopsy series that reflect the end stage of a disease process, but between 30 and 70% (depending on the primary tumor) of patients who die of cancer have liver metastases at autopsy [85].

Liver metastases generally present the histotype of the primary neoplasm. The range of gross morphology of liver metastases, their localization, as well as their number is very wide. The shape of the lesion is usually roundish; nevertheless, the metastases from colorectal adenocarcinoma larger than 3 cm commonly have cauliflower aspect [86]. The majority of metastatic lesions have ill-defined margins; however, metastases from squamous cell carcinoma and those from endocrine tumor, often roundish, present sharp margins. The site of the metastases is usually intrahepatic, prevailing within the right lobe; exceptionally the metastases may be localized on the liver capsule, owing to the intraperitoneal spread (ovarian and colonic adenocarcinomas). The metastases from poorly differentiated adenocarcinomas and from endocrine tumors are usually numerous, smaller than 2 cm, and disseminated to the whole liver [87].

The signal intensity of the metastases differs from that of the liver since their T1 and T2 relaxation times are longer, owing to the higher content of free water molecules; therefore, on T1-weighted images the signal

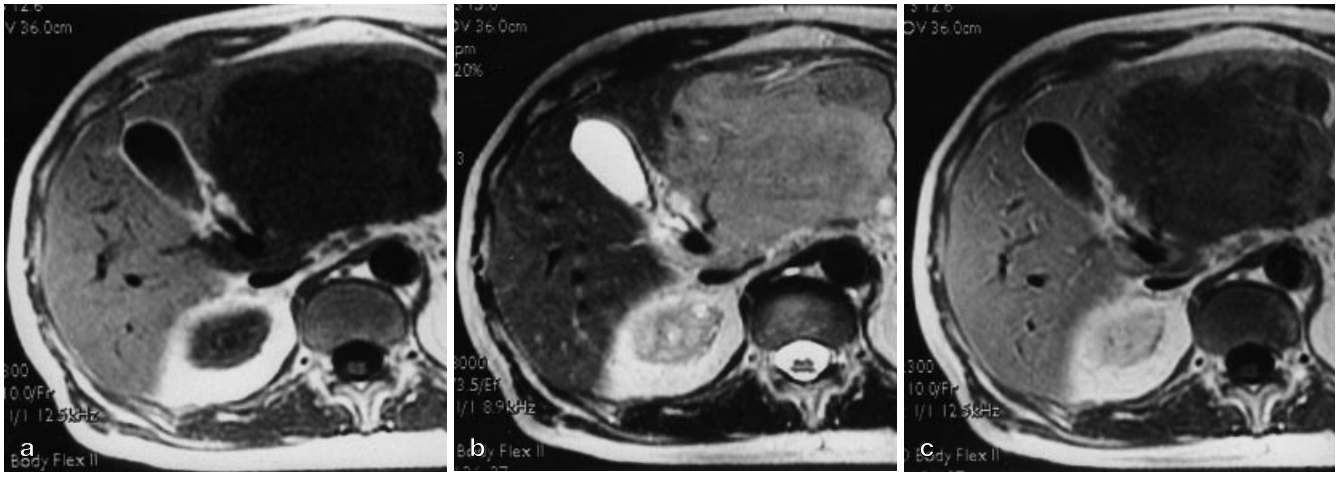

Fig. 14a–c Lymphoma. **a** On the T1-weighted image, the tumor appears as a large, homogeneously hypointense mass. **b** The lesion is hyperintense on the T2-weigted image. **c** In the delayed, contrast-enhanced image, the tumor remains hypointense to liver

intensity of the metastases is lower than that of the hepatic tissue, whereas it is higher on T2-weighted images (Fig. 15). Some peculiar pathologic conditions, however, can modify the signal intensity of the metastases. Whenever liquefactive necrosis or infectious edema is present within the metastasis, the signal intensity further increases on T2-weighted images. On the other hand, if coagulative necrosis, fibrous matrix, or calcifications are present within the metastasis, the elevated signal intensity on T2-weighted images is decreased. Finally, whenever subacute intralesional hemorrhage or particular substances, such as melanin (seen in metastases from melanoma) or mucin (produced by metastases from mucinous carcinoma of the pancreas or the ovarium), are present within the metastatic tissue, the signal intensity of T1-weighted images is increased [88, 89].

After administration of extracellular contrast agents, enhancement of the liver is stronger than that of most metastatic lesions during both the arterial and the portal phases. Hypervascular metastases, however, show strong enhancement in the arterial phase, appearing definitely hyperintense with respect to liver parenchyma [88, 90]. Large hypervascular metastases receive arterial blood mainly in the periphery of the lesion than in the worse perfused center; thus, during the arterial phase, these metastases show an intense peripheral ring of enhancement, whereas during the following phases they show a progressive enhancement into the center which is gradually separated from that of the hepatic tissue [36, 88, 91, 92, 93]. Because metastases do not contain Kupffer's cells or normal hepatocytes, no uptake of reticuloendothelial-system-target agents or hepatobiliary agents is usually seen [22, 94, 95, 96].

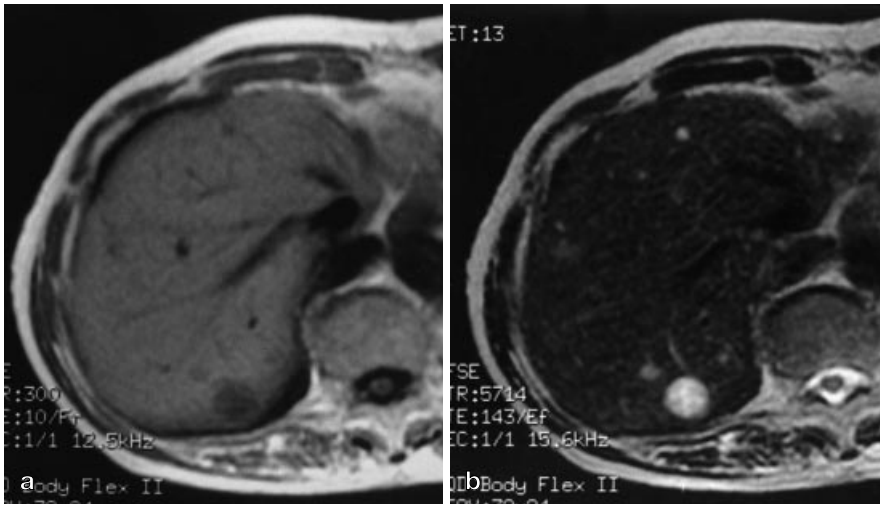

Fig. 15a, b Carcinoid metastases. **a** T1-weighted image shows small, hypointense lesions in the right hepatic lobe. **b** The lesions appear definitely hyperintense on the T2-weighted image

References

1. Bartolozzi C, Lencioni R (eds) (1999) Liver malignancies. Springer, Berlin Heidelberg New York
2. Bartolozzi C, Lencioni R, Donati F, Cioni D (1999) Abdominal MR: liver and pancreas. Eur Radiol 9: 1496–1512
3. Gourtsoyiannis N, Ros PR (eds) (2000) Radiologic–pathologic correlations. Syllabus Categorical Course ECR 2000. Eur Radiol 10 (Suppl 2)
4. Martin J, Sentis M, Zidan A et al. (1995) Fatty metamorphosis of hepatocellular carcinoma: detection with chemical shift gradient-echo MR imaging. Radiology 195: 125–130
5. Honda H, Kaneko K, Kanazawa Y et al. (1997) MR imaging of hepatocellular carcinomas: effect of Cu and Fe contents on signal intensity. Abdom Imaging 22: 60–66
6. Rofsky NM, Weinreb JC, Bernardino ME et al. (1993) Hepatocellular tumors: characterization with Mn-DPDP-enhanced MR imaging. Radiology 188: 53–59
7. Bartolozzi C, Donati F, Cioni D, Crocetti L, Lencioni R (2000) MnDPDP-enhanced MRI vs dual-phase spiral CT in the detection of hepatocellular carcinoma. Eur Radiol 10: 1697–1702
8. McFarland EG, Mayo-Smith WW, Saini S et al. (1994) Hepatic hemangiomas and malignant tumors: improved differentiation with heavily T2-weighted conventional spin-echo MR imaging. Radiology 193: 43–47
9. Sadek AG, Mitchell DG, Siegelman ES, Outwater EK, Matteucci T, Hann HW (1995) Early hepatocellular carcinoma that develops within macroregenerative nodules: growth rate depicted at serial MR imaging. Radiology 195: 753–756
10. Mattison GR, Glazer GM, Quint LE et al. (1987) MR imaging of hepatic focal nodular hyperplasia: characterization and distinction from primary malignant hepatic tumors. Am J Roentgenol 148: 711–715
11. Semelka RC, Brown ED, Ascher SM et al. (1994) Hepatic hemangiomas: a multi-institutional study of appearance on T2-weighted and serial gadolinium-enhanced gradient-echo MR images. Radiology 192: 401–406
12. Ros PR, Freeny PC, Harms SE et al. (1995) Hepatic MR imaging with ferumoxide: a multicentric clinical trial of the safety and efficacy in the detection of focal hepatic lesions. Radiology 196: 481–488
13. Wanless I, Mawdsley C, Adams R (1985) On the pathogenesis of focal nodular hyperplasia of the liver. Hepatology 5: 1194–1200
14. Shortell CK, Schwartz S (1991) Hepatic adenoma and focal nodular hyperplasia. Surg Gynecol Obstet 173: 426–431
15. Lee M, Hamm B, Saini S (1991) Focal nodular hyperplasia of the liver: MR findings in 35 proved cases. Am J Roentgenol 156: 317–320
16. Shamsi K, De Schepper A, Degryse H, Deckers F (1993) Focal nodular hyerplasia of the liver: radiologic findings. Abdom Imaging 18: 32–38
17. Vilgrain V, Flejou J, Arrive L et al. (1992) Focal nodular hyperplasia of the liver: MR imaging and pathologic correlation in 37 patients. Radiology 184: 699–703
18. Buetow PC, Pantongrag-Brown L, Buck JL et al. (1996) Focal nodular hyperplasia of the liver: imaging–pathologic correlation. Radiographics 16: 369–388
19. Rummeny E, Weissleder R, Sironi S et al. (1989) Central scars in primary liver tumors: MR features, specificity, and pathologic correlation. Radiology 171: 323–326
20. Mahfouz AE, Hamm B, Taupitz M et al. (1993) Hypervascular liver lesions. Differentiation focal nodular hyperplasia from malignant tumors with dynamic gadolinium-enhanced MR imaging. Radiology 186: 133–138
21. Bernardino ME, Young SW, Lee JKT et al. (1992) Hepatic MR imaging with Mn-DPDP: safety, image quality, and sensitivity. Radiology 183: 53–58
22. Wang C, Ahlstrom H, Ekholm S et al. (1998) Diagnostic efficacy of Mn-DPDP in MR imaging of the liver. A phase III multicentre study. Acta Radiol 38: 643–649
23. Paulson EK, McClennon JS, Washington K et al. (1994) Hepatic adenoma: MR characteristics and correlations with pathologic findings. Am J Roentgenol 163: 113–116
24. Chung KY, Mayo-Smith WW, Saini S et al. (1995) Hepatocellular adenoma: MR imaging features with pathologic correlation. Am J Roentgenol 165: 303–308
25. Kawarada Y, Mizumoto R (1983) Angiomyolipoma of the liver. Am J Gastroenterol 78: 434–436
26. Nguyen GK, Catzavelos C (1990) Solitary angiomyolipoma of the liver. Acta Cytol 34: 201–204
27. Fobbe F, Hamm B, Schwarting R (1988) Angiomyolipoma of the liver: CT, MR and ultrasound imaging. J Comput Assist Tomogr 12: 658–659
28. Hooper LD, Mergo PJ, Ros PR (1994) Multiple hepatorenal angiomyolipomas: diagnosis with fat suppression, gadolinium-enhanced MRI. Abdom Imaging 19: 549–551
29. Borzio M, Bruno S, Roncalli M et al. (1991) Liver cell dysplasia and risk of hepatocellular carcinoma in cirrhosis: a preliminary report. Br Med J 302: 1312–1315
30. Lencioni R, Bartolozzi C, Caramella D, Coscio G di (1993) Management of adenomatous hyperplastic nodules in the cirrhotic liver: US follow-up or percutaneous alcohol ablation? Abdom Imaging 18: 50–55
31. Dachmman AH, Ros PR, Goodman ZD et al. (1987) Nodular regenerative hyperplasia of the liver: clinical and radiologic observations. Am J Roentgenol 148: 717–722
32. Ferrel L, Wright T, Lake J et al. (1992) Incidence and diagnostic features of macroregenerative nodules vs small hepatocellular carcinoma in cirrhotic livers. Hepatology 16: 1372–1381
33. Wada K, Kondo F, Kondo Y (1988) Large regenerative nodules and dysplastic nodules in cirrhotic livers: a histopathologic study. Hepatology 12: 592–597
34. Watanabe S, Okita K, Harada T et al. (1983) Morphologic studies of the liver cell dysplasia. Cancer 51: 2197–2205
35. Earls JP, Theise ND, Weinreb JC et al. (1996) Dysplastic nodules and hepatocellular carcinoma: thin-section MR imaging of explanted cirrhotic livers with pathologic correlation. Radiology 201: 207–214
36. Nakashima O, Sugihara S, Kage M et al. (1995) Pathomorphologic characteristics of small hepatocellular carcinoma: a special reference to small hepatocellular carcinoma with indistict margins. Hepatology 22: 101–105
37. Ebara M, Watanabe S, Kita K et al. (1991) MR imaging of small hepatocellular carcinoma: effect of intratumoral copper content on signal intensity. Radiology 180: 617–621
38. Kitagawa K, Matsui O, Kadoya M et al. (1991) Hepatocellular carcinomas with excessive copper accumulation: CT and MR findings. Radiology 180: 623–628

39. Matsuzaki K, Sano N, Hashiguchi N, Yoshida S, Nishitani H (1997) Influence of copper on MRI of hepatocellular carcinoma. J Magn Reson Imaging 7: 478–481
40. Semelka RC, Bagley AS, Brown ED et al. (1994) Malignant lesions of the liver identified on T1- but not T2-weighted MR images at 1.5 T. J Magn Reson Imaging 4: 315–318
41. Lencioni R. Mascalchi M, Caramella D, Bartolozzi C (1996) Small hepatocellular carcinoma: differentiation from adenomatous hyperplasia with color Doppler US and dynamic Gd-DTPA-enhanced MR imaging. Abdom Imaging 21: 41–48
42. Bartolozzi C, Lencioni R, Caramella D, Paolicchi A, Russo R, Romani R (1994) The magnetic resonance and histological correlations in hepatocellular carcinoma. Radiol Med 87: 90–95
43. Inoue E, Kuroda C, Fujita M et al. (1993) MR features of various histological grades of small hepatocellular carcinoma. J Comput Assist Tomogr 17: 75–79
44. Winter T, Takayasu K, Muramatsu Y et al. (1994) Early advanced hepatocellular carcinoma: evaluation of CT and MR appearance with pathologic correlation. Radiology 192: 379–387
45. Choi BI, Lee GK, Kim ST, Han MC (1990) Mosaic pattern of encapsulated hepatocellular carcinoma: correlation of magnetic resonance imaging and pathology. Gastrointest Radiol 15: 238–240
46. Matsui O, Kadoya M, Kameyama T et al. (1991) Benign and malignant nodules in cirrhotic livers: distinction based on blood supply. Radiology 178: 493–497
47. Yamashita Y, Fan ZM, Yamamoto H et al. (1994) Spin-echo and dynamic gadolinium-enhanced FLASH MR imaging of hepatocellular carcinoma: correlation with histopathologic findings. J Magn Reson Imaging 4: 83–90
48. Hamm B, Theoni RG, Gould RG et al. (1994) Focal liver lesions: characterization with non-enhanced and dynamic contrast material enhanced MR imaging. Radiology 190: 417–423
49. Vogl TJ, Stupavsky A, Pegios W, Hammerstingl R (1997) Hepatocellular carcinoma: evaluation with dynamic and static gadobenate dimeglumine-enhanced MR imaging and histopathologic correlation. Radiology 205: 721–728
50. Larson RE, Semelka RC, Bagley AS et al. (1994) Hypervascular malignant liver lesions: comparison of various MR imaging pulse sequences and dynamic CT. Radiology 192: 393–399
51. Buetow PC, Buck JL, Ros PR et al. (1994) Malignant vascular tumors of the liver: radiologic–pathologic correlation. Radiographics 14: 153–l66
52. Peterson MS, Baron RL, Murakami T (1996) Hepatic malignancies: usefulness of acquisition of multiple arterial and portal venous phase images at dynamic gadolinium-enhanced MR imaging. Radiology 201: 337–345
53. Itoh K, Nishimura K, Togashi K et al. (1987) Hepatocellular carcinoma: MR imaging. Radiology 164: 21–25
54. Kadoya M, Matsui O, Takashima T, Nonomura A (1992) Hepatocellular carcinoma: correlation of MR imaging and histopathologic findings. Radiology 183: 819–825
55. Soyer P, Clément de Givry S, Gueye C et al. (1996) Detection of focal hepatic lesions with MR imaging: prospective comparison of T2-weighted fast spin echo with and without fat suppression, T2-weighted breath-hold fast spin echo, and gadolinium chelate enhanced 3D gradient-recalled imaging. Am J Roentgenol 166: 1115–1121
56. Bartolozzi C, Lencioni R, Caramella D, Palla A, Bassi AM, Candio G di (1996) Small hepatocellular carcinoma: detection with US, CT, MR imaging, DSA, and Lipiodol-CT. Acta Radiol 37: 69–74
57. Muramatsu Y, Nawano S, Takayasu K et al. (1991) Early hepatocellular carcinoma: MR imaging. Radiology 181: 209–213
58. Yamashita Y, Fan ZM, Yamamoto H et al. (1993) Sclerosing hepatocellular carcinoma: radiologic findings. Abdom Imaging 18: 347–351
59. Murakami T, Baron RL, Peterson MS (1996) Hepatocellular carcinoma: MR imaging with mangafodipir trisodium (Mn-DPDP). Radiology 200: 69–77
60. Vogl TJ, Hamm B, Schnell B et al. (1993) Mn-DPDP enhancement patterns of hepatocellular lesions on MR images. J Magn Reson Imaging 3: 51–56
61. Ros PR, Buck JL, Comdr LT, Goodman ZD et al. (1988) Intrahepatic cholangiocarcinoma: radiology–pathologic correlation. Radiology 167: 689–693
62. Tani K, Kubota Y, Yamaguchi T et al. (1991) MR imaging of peripheral cholangiocarcinoma. J Comput Assist Tomogr 15: 975–978
63. Soyer P, Bluemke DA, Sibert A, Laissy JP (1995) MR imaging of intrahepatic cholangiocarcinoma. Abdom Imaging 20: 126–130
64. Guthrie JA, Ward J, Robinson PJ (1996) Hilar cholangiocarcinoma: T2-weighted spin-echo and gadolinium enhanced FLASH MR imaging. Radiology 201: 347–351
65. Adjei ON, Tamura S, Sugimara H et al. (1995) Contrast enhanced MR imaging of intrahepatic cholangiocarcinoma. Clin Radiol 50: 6–10
66. Choi BI, Han JK, Shin YM et al. (1995) Peripheral cholangiocarcinoma: comparison of MRI with CT. Abdom Imaging 20: 357–360
67. Murakami T, Nakamura H, Tsuda K et al. (1995) Contrast-enhanced MR imaging of intrahepatic cholangiocarcinoma: pathologic correlation study. J Magn Reson Imaging 5: 165–170
68. Craig JR, Peters RL, Edmondson HA et al. (1980) Fibrolamellar carcinoma of the liver: a tumor of adolescents and young adults with distinctive clinicopathologic features. Cancer 46: 372–379
69. Titelbaum DS, Burke DR, Meranze SG, Saul SH (1988) Fibrolamellar hepatocellular carcinoma: pitfalls in nonoperative diagnosis. Radiology 167: 25–30
70. Wong LK, Link DP, Frey CF (1982) Fibrolamellar hepatocarcinoma: radiology, management and pathology. Am J Roentgenol 139: 172–175
71. Friedman AC, Lichtenstein JE, Goodman Z et al. (1985) Fibrolamellar hepatocellular carcinoma. Radiology 157: 583–587
72. Lefkowich JH, Muschel R, Price JB et al. (1983) Copper and copper-binding protein in fibrolamellar liver cell carcinoma. Cancer 51: 97–100
73. Brandt DJ, Johnson CD, Stephens DH, Weiland LH (1988) Imaging of fibrolamellar hepatocellular carcinoma. Am J Roentgenol 151: 295–299
74. Corrigan K, Semelka RC (1995) Dynamic contrast-enhanced MR imaging of fibrolamellar hepatocellular carcinoma. Abdom Imaging 20: 122–125
75. Weiss JW, Enzinger FM (1982) Epithelioid hemangioendothelioma: a vascular tumor often mistaken for a carcinoma. Cancer 50: 970–981
76. Radin DR, Craig JR, Colletti PM et al. (1988) Hepatic epithelioid hemangioendothelioma. Radiology 169: 145–148
77. Kelleher MB, Iwatsuki S, Sheahan DG (1989) Epithelioid hemangioendothelioma of the liver. Clinicopathological correlation of 10 cases trated by orthotopic liver transplantation. Am J Surg Pathol 13: 999–1008

78. Miller WJ, Dodd GD III, Federle MP, Baron RL (1992) Epithelioid hemangioendothelioma of the liver: imaging findings with pathologic correlation. Am J Roentgenol 159: 53–57
79. Ito Y, Kojiro M, Nakashima T et al. (1988) Pathomorphologic characteristics of 102 cases of thorotrast-related hepatocellular carcinoma, cholangiocarcinoma, and hepatic angiosarcoma. Cancer 62: 1153–1162
80. Marti-Bonmati L, Ferrer D, Menor F et al. (1993) Hepatic mesenchymal sarcoma: MRI findings. Abdom lmaging 18: 176–179
81. Ryan J, Straus DJ, Lange C et al. (1988) Primary lymphoma of the liver. Cancer 61: 370–375
82. Shirkhoda A, Ros PR, Farah J et al. (1990) Lymphoma of the solid abdominal viscera. Radiol Clin North Am 28: 785–799
83. Weissieder R, Stark DD, Elizondo G et al. (1988) MRI of hepatic lymphoma. Magn Reson lmaging 6: 675–681
84. Fukuya T, Honda H, Murata S et al. (1993) MRI of primary lymphoma of the liver. J Comput Assist Tomogr 17: 596–598
85. Pickren JK, Tsukada Y, Lane WW (1082) Liver metastasis. analysis of autopsy data. In: Weiss L, Gilbert HA (eds) Liver metastasis. Hall, Boston, pp 2–18
86. Wagner JS, Adson MA, Van Heerden JA et al. (1984) The natural history of hepatic metastases from colorectal cancer. Ann Surg 199: 502–508
87. Outwater E, Tomaszewski E, Daly JM et al. (1991) Hepatic colorectal metastases: correlation of MR imaging and pathologic appearance. Radiology 180: 327–332
88. Mahfouz AE, Hamm B, Mathieu D (1996) Imaging of metastases to the liver. Eur Radiol 6: 607–614
89. Kokubo T, Itai Y, Ohtomo K et al. (1988) Mucin-hypersecreting intrahepatic biliary neoplasms. Radiology 168: 609–614
90. Soyer P, Gueye C, Somerveille E et al. (1995) MR diagnosis of hepatic metastases from neuroendocrine tumors versus hemangiomas: relative merits of dynamics gadolinium chelate-enhanced gradient-recalled echo and unenhanced spin-echo images. Am J Roentgenol 165: 1407–1413
91. Hamm B, Mahfouz AE, Taupitz M et al. (1997) Liver metastases: improved detection with dynamic gadolinium-enhanced MR imaging? Radiology 202: 677–682
92. Reinig JW, Dwyer AJ, Miller DL et al. (1989) Liver metastases: detection with MR Imaging at 0.5 and 1.5 T. Radiology 170: 149–153
93. Fretz CJ, Stark DD, Metz CE et al. (1990) Detection of hepatic metastases: comparison of contrast-enhanced CT, unenhanced MR imaging, and iron-oxide enhanced MR imaging. Am J Roentgenol 155: 763–770
94. Hagspiel KD, Neidl KFW, Eichenberger AC et al. (1995) Detection of liver metastases: comparison of superparamagnetic iron-oxide enhanced and unenhanced MR imaging at 1.5 T with dynamic CT, intraoperative US, and percutaneous US. Radiology 196: 471–478
95. Senéterre E, Taourel P, Bouvier Y et al. (1996) Detection of hepatic metastases: ferumoxide-enhanced MR imaging versus unenhanced MR imaging and CT during arterial portography. Radiology 200: 785–792
96. Lencioni R, Donati F, Cioni D, Paolicchi A, Cicorelli A, Bartolozzi C (1998) Detection of colorectal liver metastases: prospective comparison of unenhanced and ferumoxides-enhanced magnetic resonance imaging at 1.5 T, dual-phase spiral CT, and spiral CT during arterial portography. MAGMA 7: 76–87